Experimental assessment of an unknown-input estimator for a nonlinear wave energy converter

Experimental assessment of an unknown-input estimator for a nonlinear wave energy converter [*]

Edoardo Pasta [*] Guglielmo Papini [*] Fabio Carapellese [*]
Nicolás Faedo [*] John V. Ringwood [**]

[*] *Marine Offshore Renewable Energy Lab., Department of Mechanical and Aerospace Engineering, Politecnico di Torino, Turin, Italy. (e-mail: edoardo.pasta@polito.it).*
[**] *Centre for Ocean Energy Research, National University of Ireland, Maynooth, Co. Kildare, Ireland.*

Abstract: In the wave energy field, one of the main challenges towards commercialisation of wave energy devices is the development of suitable control laws, able to maximise the absorbed energy while guaranteeing effective satisfaction of any required physical constraint. However, one of the main characteristics of this optimal control problem is that the system behaviour is strongly influenced by the external (uncontrollable) input arising from the wave source, *i.e.* the wave excitation, which is often unmeasurable. As such, computation of optimal control solutions for WEC systems requires availability of instantaneous knowledge of the wave excitation, and hence input-unknown estimators are developed within the control loop. State-of-the-art estimation strategies are based on the knowledge of control-oriented linearized models of the system, often neglecting the influence of nonlinear phenomena within the system description. We propose, in this paper, an approach inspired by disturbance observer-based control, able to accommodate well-known hydrodynamic nonlinear effects in the process of estimating the unknown excitation force acting on the device. This strategy, which in contrast to the usually applied estimators does not require an implicit/explicit model of the wave excitation force, is tested on a hardware-in-the-loop facility in different sea state conditions, to realistically assess its performance in terms of estimation error and delay. The experimental appraisal show satisfactory results in terms of normalized root mean square error and average delay, which, together with the simplicity of the method, positions the proposed strategy as a promising candidate for hardware implementations in real environments.

Keywords: Wave energy; unknown-input estimation; nonlinear systems; experimental assessment; energy-maximising control; disturbance observer-based control.

1. INTRODUCTION

Among state-of-the-art energy extraction techniques, *wave energy converters* (WECs) have a remarkable untapped potential (Mattiazzo, 2019), capable of greatly supporting the pathway towards energy decarbonisation. Nonetheless, wave energy technology has not reached a level of maturity able to enable full commercialisation, especially due to its currently high *levelised cost of energy* (LCoE) (Guo and Ringwood, 2021). In this context, one of the key stepping stones towards a competitive and appealing LCoE is the development of suitable control strategies (Ringwood, 2020). The WEC control problem, whose solution is crucial for economic viability, can be written in terms of a constrained and energy-maximising problem (Hals et al., 2011; Faedo et al., 2017). In fact, any developed strategy should maximise the absorbed energy over a certain time window $\mathcal{T}$, while, at the same time, respecting any

possible constraint on the device, effectively minimising potential failures of the conversion system. These goals and requirements are usually translated into an *optimal control problem* (OCP), whose definition is virtually always *model-based*. In fact, a simplified control-oriented version of the system model is usually adopted to describe the WEC dynamics, and propagate it through future time instants within the window $\mathcal{T}$, over which the control action is optimised. However, these models are often subject to simplifications (*e.g.* linearisation around an equilibrium position (Carapellese et al., 2022a), or the omission of nonlinear contributions at the modeling stage (Penalba et al., 2017)), and thus affected by inaccuracies that, if not properly considered (Faedo et al., 2022a), could dramatically interfere with the synthesis of the elements constituting the control loop. Moreover, such systems are highly influenced by an external (uncontrollable) force, *i.e.* the wave excitation force, which effectively represents the force exerted by the incoming wave field on the WEC system. Most of the strategies adopted to solve the OCP require the knowledge of this contribution (Li and Belmont, 2014;

Table 1. Full-scale dimensions of the emulated flap-type WEC.

Parameter	Value (m)
D1	2.2
D2	10.0
D3	18.0
D4	8.0

Garcia-Violini et al., 2020; Carapellese et al., 2022b), since it directly affects the optimality condition (Faedo et al., 2022c). For this reason, among the elements that need to be designed to develop the control loop, a crucial role is that played by so-called *unknown-input estimators*, able to provide an instantaneous estimate of the (generally non measurable) wave excitation force signal (Peña-Sanchez et al., 2020; Abdelrahman and Patton, 2020; Abdelkhalik et al., 2016; Zhang et al., 2020). Since the development of such estimators is also model-based, the degree of fidelity of the employed model has, naturally, an impact on the outcome of the estimation process. Motivated by the need of estimation strategies able to incorporate nonlinear contributions inside the model adopted in the synthesis stage, we develop and test, within this paper, an unknown-input estimator able to accomodate well-known hydrodynamic nonlinear effects which characterize wave energy devices. The presented estimation process is tested on an *hardware-in-the-loop* (HiL) system to assess the capabilities of estimating the unknown signal in real-time.

The remainder of the paper is organized as follows. In Sect. 2, the model used to describe the WEC dynamics is presented, together with the set of assumptions adopted. Sect. 3 is aimed at describing the HiL facility used in the results assessment. In Sect. 4, the approach for the development of the proposed unknown-input strategy is introduced, highlighting its validity and design procedure, while Sect. 5 present, and analyses, the experimental results. Finally, in Sect. 6, conclusions are presented regarding main capabilities of the strategy, highlighting the scope of potential applications.

2. WEC MODELING

Among WEC technologies, one of the possible concepts is the oscillating wave surge converter (OWSC, also known as a 'flap'), which converts the energy coming from the wave motion by damping the torque exerted on a flap by virtue of the wave field (Henry et al., 2010). Its structure is composed of a flap placed on the seabed, connected to a Power Take-Off (PTO) system, and free to rotate about the axis of the latter. The generator shaft constitutes the flap hinge. A schematic representation can be seen in Fig. 1, together with the full-scale dimensions of the WEC emulated in this paper in Table 1.

The dynamics of these devices can be modeled by means of potential flow theory assumptions, considering a single degree of freedom [1] (DoF) as:

$$I_z \ddot{z}(t) = f_r(t) + f_{hr}^l(t) + f^{nl}(t) + f_{ex}(t) - f_{PTO}(t), \quad (1)$$

where $I_z \in \mathbb{R}^+$ is the device inertia, $t \mapsto z(t) \in \mathbb{R}$ is the WEC angular displacement, $t \mapsto f_r(t) \in \mathbb{R}$ is the

---

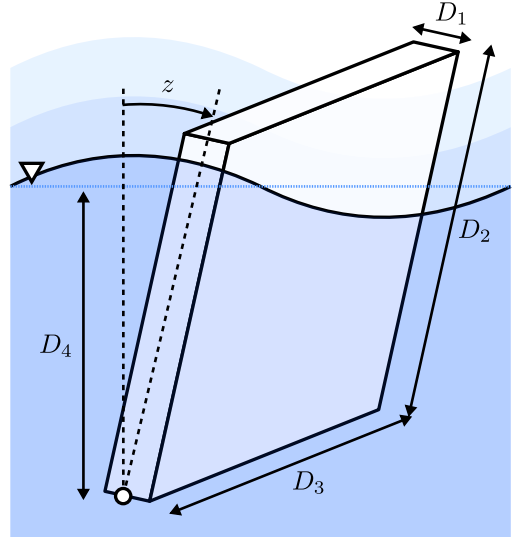[1] Note that similar arguments can be made for multi-DoF devices (see, for instance, (Folley, 2016)).

Fig. 1. Flap-type WEC schematic.

radiation torque, $t \mapsto f_{hr}^l(t) \in \mathbb{R}$ is the linearised hydrostatic restoring torque (where the Jacobian linearisation is usually performed about the equilibrium position $z = 0$), $t \mapsto f^{nl}(t) \in \mathbb{R}$ represents potential sources of nonlinearity, $t \mapsto f_{ex}(t) \in \mathbb{R}$ is the wave excitation torque, and $t \mapsto f_{PTO}(t) \in \mathbb{R}$ denotes the control torque applied by the PTO. In control-oriented modeling, f_r is usually split [2] in two contributions: the first one corresponds to an effect of added mass, while the second one, which following the so-called Cummins' equation (Cummins, 1962), is represented by a convolution integral, is usually parameterised by a state space representation (Peña-Sanchez et al., 2019). The linearized restoring contribution f_{hr}^l, instead, is modeled as a stiffness term, proportional to the WEC displacement from the equilibrium position. Finally, the excitation torque term f_{ex} is usually modeled as a Gaussian process, to take into account the stochastic nature of the wave phenomena (Merigaud and Ringwood, 2018).

Potential sources of nonlinearity that typically affect wave energy converters are viscous effects, nonlinear restoring contributions, or other forms of nonlinearity that depend on either the device wetted surface, or any internal state (*e.g.* velocity) (Penalba et al., 2017). In this paper, we consider, as nonlinear torque acting on the flap device, a nonlinear viscous effect f_v^{nl}, written in terms of the following Morison-like equation:

$$f_v^{nl} = -\beta_v \dot{z}|\dot{z}|, \quad (2)$$

where β_v is the viscous coefficient.

Having defined the torques acting on the WEC as in (1), the only external force contributions on the system are the excitation torque f_{ex}, and the control torque f_{PTO} applied by the PTO. Letting x be the state-vector associated with the WEC system, we can write the dynamical equation, describing the WEC motion, as:

$$g_{\text{WEC}} : \begin{cases} \dot{x} = Ax + B(f_{ex} - f_{PTO} + f^{nl}(x)), \\ \dot{z} = Cx, \end{cases} \quad (3)$$

with the triple (A, B, C) minimal and of appropriate dimensions, and where $f^{nl} : \mathbb{R}^n \to \mathbb{R}$ (with n the

---

[2] From now on, the dependence on t is dropped when clear from the context.
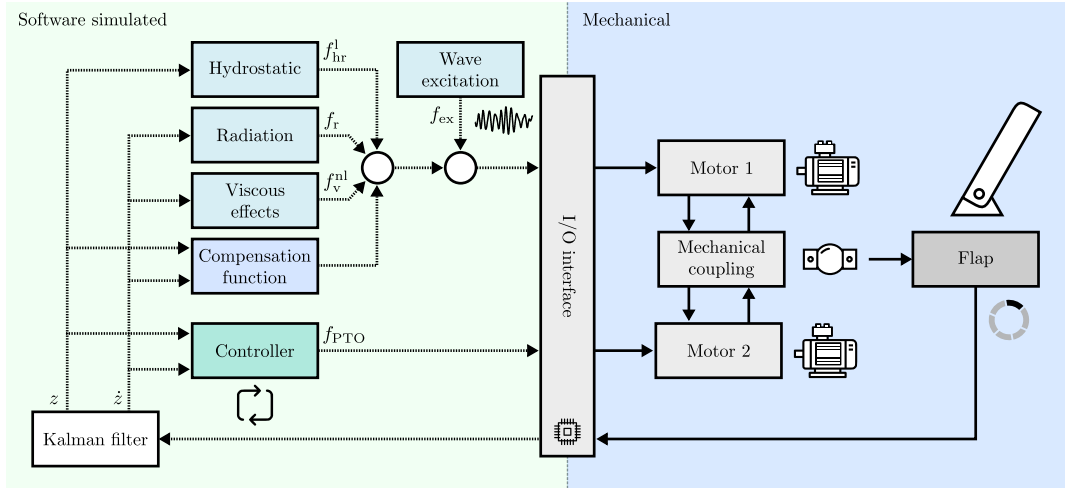
Fig. 2. COER flap-type HiL scheme (adapted from (Faedo et al., 2022d)).

dimension of (3)) describes, without any loss of generality, the (purely) nonlinear effects acting on the system, *i.e.* $\frac{\partial f^{nl}}{\partial x}\big|_{x=0} = 0$. When the system is linearized about $x = 0$, the associated linear representation becomes:

$$g_{\mathrm{WEC}}^l : \begin{cases} \dot{x} = Ax + B(f_{ex} - f_{PTO}), \\ \dot{z} = Cx, \end{cases} \qquad (4)$$

For the purposes of the presented paper, we assume also here that g_{WEC}^l is internally stable in the Lyapunov sense, and minimum-phase. It is also important to note that, for g_{WEC}^l, the transfer function $G_0(s) = C(s\mathbb{I} - A)^{-1}B$ can be defined.

3. OWSC WEC HIL

The assessment for the estimator designed within this paper is performed by means of a HiL system, which is located within the facilities of the Centre for Ocean Energy Research, Maynooth University, Ireland. The HiL system emulates a 1/30th scale of OWSC WEC (for a more comprehensive description of the system, the reader is referred to (Faedo et al., 2022d)). A schematic of both hardware and software elements constituting the rig is presented in Fig. 2. The HiL system is composed of two mechanically coupled servo motors (*Panasonic MSME504G1G*), each equipped with an independent driver (*Panasonic MFD-HTA464*). The coupling is performed by means of a flap-like structure, whose inertia can be changed by means of additional weights attached to the flap, to emulate different WEC inertial characteristics.

The first motor (M1) is used to emulate the hydrodynamic forces impacting the WEC device, and can be modeled by the user according to the formulation presented in Eq. (1). As mentioned in Sect. 2, apart from the linear contribution, we implement the nonlinearity given by the nonlinear viscous effect within the flap HiL dynamics (Eq. (2)). The second motor (M2) acts as the WEC PTO, exerting the control torque. As it is possible to notice from Fig. 2, an input/output (I/O) interface is present (*National Instruments PCIe-6343* acquisition board), while any software-emulated component in the data acquisition process is implemented in real-time MATLAB SIMULINK®. Apart from the WEC system dynamics and control, two additional

blocks in the HiL schematic are noteworthy. The first one is a Kalman filter, which is used to filter the angular displacement of the flap structure measured by an encoder, also providing an estimate of the flap angular velocity. The second one is, instead, the 'compensation function', whose aim is the minimisation of the error between the actual motion of M1 and the desired WEC behaviour. This block has an important role in the HiL scheme, since it is responsible for compensating any intrinsic dynamics of the rig, which do not represent any specific (desired) WEC behaviour.

4. UNKNOWN-INPUT ESTIMATOR: WORKING PRINCIPLE AND DESIGN

As mentioned in Sect. 1, the wave excitation torque f_{ex}, *i.e.* the torque exerted by the incoming wave field on the WEC system, is an external (uncontrollable) contribution that is virtually always unmeasurable. Moreover, the knowledge of present (and future) values of f_{ex} is of paramount importance for the proper solution of the WEC optimal control problem (for the contributions that this term has on both absorbed energy and constraint handling capabilities (Pasta et al., 2022)). This motivates the need for an unknown-input estimator.

Popular estimation approaches are typically based upon an internal model of the wave process (*e.g.* a harmonic model (Peña-Sanchez et al., 2020; Davis and Fabien, 2020)) and, for this reason, their design parameters normally require re-tuning according to the different sea states that can potentially be faced by the device. However, an alternative approach, which is inspired by disturbance observer-based control and that does not require implicit/explicit
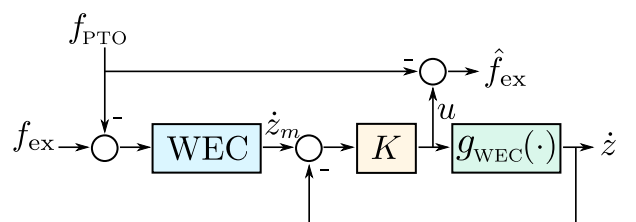

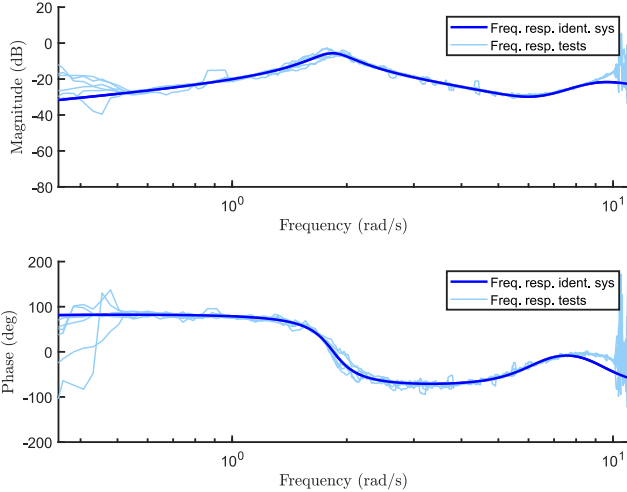Fig. 3. Estimator loop representation.

Fig. 4. Tests frequency responses and identified G_0.

representations of f_{ex}, can be adopted (Faedo et al., 2022b). Following this approach, with the right setting, an unknown-input strategy, able to accommodate well-known hydrodynamic nonlinear effect, can be developed, as discussed in the following.

A schematic representation of the loop characterising the estimation approach can be observed in Fig. 3. In this scheme, the WEC block corresponds to the real WEC system (that in the following section will be substituted by the HiL), $\dot{z}_m$ is the measured velocity, $u = f_{ex} - f_{PTO}$ is the total external (controllable and uncontrollable) torque, g_{WEC} (as described in Sect. 2) is the WEC model describing the relation $u \mapsto \dot{z}$, while K is the 'control' block used by the unknown-input estimator. Through K, the estimator tracks $\dot{z}_m$ ideally achieving:

$$\lim_{t \to \infty} \|\dot{z} - \dot{z}_m\| = 0. \qquad (5)$$

It must be noticed that, with this structure, g_{WEC} can be nonlinear if any f^{nl} is modeled. This enables the possibility to take into account the system nonlinearities in the process, to enhance the estimation. Within this paper, the tracking controller K is designed by means of the Youla-Kučera parametrisation, on the basis of the linear model $G_0(s)$ of the WEC system described in Eq. (3), *i.e.*:

$$K(s) = \frac{Q(s)}{1 - Q(s)G_0(s)}, \qquad (6)$$

with $Q(s)$ designed following the principle of plant-inversion, to achieve reference tracking, through the shaping filter $F_Q(s)$:

$$Q(s) = F_Q(s)G_0^{-1}(s), \qquad (7)$$

$$F_Q(s) = \frac{\omega_c/q_f s}{s^2 + \omega_c/q_f s + \omega_c^2}, \qquad (8)$$

where, in Eq. (8), ω_c is the band-pass filter cut-off frequency, and q_f is the shaping factor.

In this paper, we perform a system identification process to obtain the total HiL system transfer function G_0, to include in the linear representation, used in the corresponding estimator design, any potential dynamics not perfectly compensated by the compensation function implemented inside the HiL platform. To do that, a set of *multisine* signals (with box spectrum in the range of frequencies of

Table 2. List of tested sea states.

Wave ID	H_s (m)	T_p (s)	$H_s^{scal.}$ (m)	$T_p^{scal.}$ (s)
S1	2	8	0.067	1.461
S2	3	10	0.100	1.826
S3	2.5	6	0.083	1.095
S4	2.5	9	0.083	1.643

interest, random phases, and different amplitude values (Schoukens and Ljung, 2019)) has been applied to the PTO axis (acting as the total external contribution u), via motor M2. On the basis of the average frequency response of the system to the different multisine signals, a minimal parametric model is identified, consistent with the physical WEC properties discussed in Sect. 2. It is important to note that the presence of the shaping filter in the design enables the possibility of rejecting noise contributions at frequencies which are higher than those of interest. Moreover, since no assumption has been made in the design stage about the f_{ex} contribution to be tracked, the same estimator design should be suitable for different wave conditions, as long as the closed-loop bandwidth is sufficiently large, in contrast to other state-of-the-art estimation techniques.

5. EXPERIMENTAL RESULTS

Following the design and synthesis of the estimator in terms of the loop in Fig. 3, the proposed technique is deployed in the HiL rig. To assess the performance of the estimator online, four sea states are considered, each one characterised in terms of two different realisations. Table 2 presents a list of all the considered wave conditions.

To assess the performance of the estimator, the estimated excitation torque $\hat{f}_{ex}$ is compared with the real excitation force f_{ex}, which, in the HiL, is provided by M1. The comparison is performed in terms of the *normalized root mean square error* (NRMSE), and delay between the target and estimated signal (Δt). The NRMSE is computed as:

$$\text{NRMSE} = \sqrt{\frac{\sum_{k=1}^{L}(f_{ex}(k) - \hat{f}_{ex}(k))^2}{\sum_{k=1}^{L} f_{ex}(k)^2}}, \qquad (9)$$

where $f_{ex}(k)$ and $\hat{f}_{ex}(k)$ are the values of f_{ex} and $\hat{f}_{ex}$ at the k-th time instant, and L is the number of signal values. The delay between the estimated and target excitation torques is computed by finding the lag which maximises the correlation between $f_{ex}(k)$ and $\hat{f}_{ex}(k)$, *i.e.*

$$\text{Corr}(k_{lag}) = \sum_{k=1}^{L-1} f_{ex}(k)\hat{f}_{ex}(k + k_{lag}), \qquad (10)$$

$$k_{lag}^{\star} = \arg \max_{k_{lag}}(\text{Corr}(k_{lag})), \qquad (11)$$

$$\Delta t = T_s k_{lag}^{\star}, \qquad (12)$$

where $k_{lag} \in \mathbb{Z}$ is a possible delay between the two considered signals, $\text{Corr}(k_{lag})$ is the correlation function, $k_{lag}^{\star}$ is the lag that maximises the correlation, and T_s is the sampling time.

The results of the performance assessment in the four sea conditions are shown in Table 3, where the subscript of the Wave ID identifies the realisation. Note that the average NRMSE among the tests is around 9.8%, while the average delay is about 0.0085s. Moreover, the worst
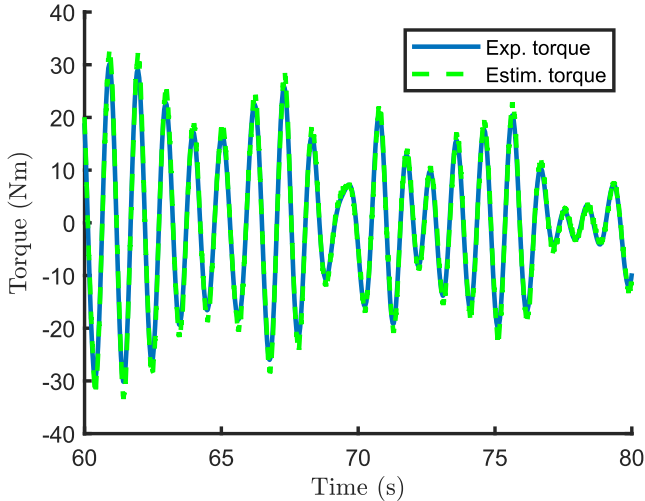
Fig. 5. Estimator tested with Wave ID S3: torque valida-
tion.

performances correspond to sea state S3, which is the
one with highest significant wave height. This result can
be explained in terms of the controller used to track
the velocity inside the estimation loop. This controller
is based on the linear version of the system model G_0,
which becomes less representative of the WEC process
as the wave height increases (*i.e.* as the system departs
from its equilibrium position). Moreover, for the sake of
completeness, it must be highlighted that the estimation
strategy is deployed on the hardware and run in real-time
successfully at a sampling frequency of 1 kHz.

Finally, a comparison in the time domain of target and
estimated signals is reported in Fig. 5 for $S3_1$. Note that
the estimation strategy is able to estimate the target wave
excitation torque with negligible error most of the time,
showing good potential for control-oriented applications,
in which precise information on the applied force is of
paramount importance (especially in terms of instanta-
neous phase-locking - see *e.g.* (Faedo et al., 2021)). More-
over, since the entire estimation strategy is based on the
concept of tracking the real measured velocity, a compar-
ison between $\dot{z}_m$ (in blue) and $\dot{z}$ (in green) is presented in
Fig. 6. The velocity is properly tracked, corroborating the
results concerning the estimated torque.

6. CONCLUSIONS

In this paper, we propose a strategy to design an unknown-
input estimator able to include the knowledge of nonlin-
earities that usually affect wave energy converters. The
estimator is based on the concept of disturbance observer-

Table 3. Estimation results: estimation
NRMSE and delay.

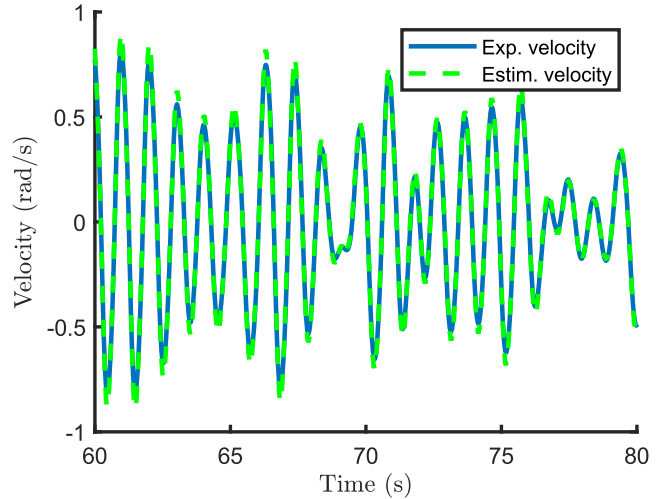| Wave ID	NRMSE (%)	Δt (s)
$S1_1$	9.66	0.008
$S1_2$	9.76	0.007
$S2_1$	10.66	0.010
$S2_2$	11.17	0.011
$S3_1$	8.92	0.007
$S3_2$	8.60	0.007
$S4_1$	10.43	0.009
$S4_2$	9.90	0.009

Fig. 6. Estimator tested with Wave ID S3: velocity track-
ing.

based control, and, in the process of estimating the exci-
tation torque, it tracks the measured WEC velocity. The
performance of the estimation strategy are tested in real-
time on a facility that emulates the behaviour of a OWSC
device, after identification of a representative linear model
of the system through prior tests. Four sea conditions are
tested, each one characterised in terms of two different
wave realisations. The experimental results show an av-
erage NRMSE of about 9.8%, and an average estimation
delay of 0.0085s. As demonstrated by the tests, the simplic-
ity of the proposed approach allows straightforward real-
time hardware implementation, with satisfactory results
both in terms of error, and delay between estimated and
target excitation torque signal. Moreover, in contrast to
state-of-the-art approaches, a single tuning for all the
different wave conditions is employed, since no assumption
is made on the model that describes the contribution to
be estimated. Future work will evaluate the incorporation
of more sophisticated control-oriented models within the
design and synthesis of the adopted estimator, including
nonlinear static and dynamic Froude-Krylov effects (which
are considered to be linear, *i.e.* separable, within this pa-
per), by exploiting the (parametric) data-based modelling
approach presented in (Faedo et al., 2022a).

REFERENCES

Abdelkhalik, O., Shangyan Zou, Bacelli, G., Robinett,
R.D., Wilson, D.G., and Coe, R.G. (2016). Estima-
tion of excitation force on wave energy converters us-
ing pressure measurements for feedback control. In
OCEANS 2016 MTS/IEEE Monterey, 1–6. IEEE. doi:
10.1109/OCEANS.2016.7761227.

Abdelrahman, M. and Patton, R. (2020). Observer-Based
Unknown Input Estimator of Wave Excitation Force
for a Wave Energy Converter. *IEEE Transactions on
Control Systems Technology*, 28(6), 2665–2672. doi:
10.1109/TCST.2019.2944329.

Carapellese, F., Pasta, E., Faedo, N., and Giorgi, G.
(2022a). Dynamic analysis and performance assessment
of the Inertial Sea Wave Energy Converter (ISWEC)
device via harmonic balance. In IFAC (ed.), *IFAC-
PapersOnLine*, volume 55, 439–444. Lyngby, Denmark.
doi:10.1016/j.ifacol.2022.10.467.

Carapellese, F., Pasta, E., Paduano, B., Faedo, N., and Mattiazzo, G. (2022b). Intuitive LTI energy-maximising control for multi-degree of freedom wave energy converters: The PeWEC case. *Ocean Engineering*, 256, 111444. doi:10.1016/j.oceaneng.2022.111444.

Cummins, W. (1962). The impulse response function and ship motions. Technical Report 1661. Technical report, Department of the Navy, David Taylor model basin, Washington DC.

Davis, A.F. and Fabien, B.C. (2020). Wave excitation force estimation of wave energy floats using extended Kalman filters. *Ocean Engineering*, 198, 106970. doi:10.1016/j.oceaneng.2020.106970.

Faedo, N., Giorgi, G., Ringwood, J.V., and Mattiazzo, G. (2022a). Optimal control of wave energy systems considering nonlinear Froude–Krylov effects: control-oriented modelling and moment-based control. *Nonlinear Dynamics*, 109(3), 1777–1804. doi:10.1007/s11071-022-07530-3.

Faedo, N., Bussi, U., Peña-Sanchez, Y., Windt, C., and Ringwood, J.V. (2022b). A Simple and Effective Excitation Force Estimator for Wave Energy Systems. *IEEE Transactions on Sustainable Energy*, 13(1), 241–250. doi:10.1109/TSTE.2021.3108576.

Faedo, N., Carapellese, F., Pasta, E., and Mattiazzo, G. (2022c). On the principle of impedance-matching for underactuated wave energy harvesting systems. *Applied Ocean Research*, 118, 102958. doi:10.1016/j.apor.2021.102958.

Faedo, N., Mosquera, F.D., Evangelista, C.A., Ringwood, J.V., and Puleston, P.F. (2022d). Preliminary experimental assessment of second-order sliding mode control for wave energy conversion systems. In *Proceedings of the 2022 Australian and New Zealand Control Conference*. Gold Coast, Australia.

Faedo, N., Olaya, S., and Ringwood, J.V. (2017). Optimal control, MPC and MPC-like algorithms for wave energy systems: An overview. *IFAC Journal of Systems and Control*, 1, 37–56. doi:10.1016/j.ifacsc.2017.07.001.

Faedo, N., Peña-Sanchez, Y., and Ringwood, J.V. (2021). Receding-Horizon Energy-Maximising Optimal Control of Wave Energy Systems Based on Moments. *IEEE Transactions on Sustainable Energy*, 12(1), 378–386. doi:10.1109/TSTE.2020.3000013.

Folley, M. (2016). *Numerical modelling of wave energy converters: state-of-the-art techniques for single devices and arrays.* Elsevier. doi:10.1016/C2014-0-04006-3.

Garcia-Violini, D., Peña-Sanchez, Y., Faedo, N., and Ringwood, J.V. (2020). An Energy-Maximising Linear Time Invariant Controller (LiTe-Con) for Wave Energy Devices. *IEEE Transactions on Sustainable Energy*, 11(4), 2713–2721. doi:10.1109/TSTE.2020.2971392.

Guo, B. and Ringwood, J.V. (2021). A review of wave energy technology from a research and commercial perspective. *IET Renewable Power Generation*, 15(14), 3065–3090. doi:10.1049/rpg2.12302.

Hals, J., Falnes, J., and Moan, T. (2011). Constrained Optimal Control of a Heaving Buoy Wave-Energy Converter. *Journal of Offshore Mechanics and Arctic Engineering*, 133(1). doi:10.1115/1.4001431.

Henry, A., Doherty, K., Cameron, L., Doherty, R., and Whittaker, T. (2010). Advances in the Design of the Oyster Wave Energy Converter. In *Marine Renewable and Offshore Wind Energy*, 119–128. doi:10.3940/rina.mre.2010.14.

Li, G. and Belmont, M.R. (2014). Model predictive control of sea wave energy converters – Part I: A convex approach for the case of a single device. *Renewable Energy*, 69, 453–463. doi:10.1016/j.renene.2014.03.070.

Mattiazzo, G. (2019). State of the Art and Perspectives of Wave Energy in the Mediterranean Sea: Backstage of ISWEC. *Frontiers in Energy Research*, 7. doi:10.3389/fenrg.2019.00114.

Merigaud, A. and Ringwood, J.V. (2018). Free-Surface Time-Series Generation for Wave Energy Applications. *IEEE Journal of Oceanic Engineering*, 43(1), 19–35. doi:10.1109/JOE.2017.2691199.

Pasta, E., Papini, G., Faedo, N., Mattiazzo, G., and Ringwood, J. (2022). On optimization-based strategies in data-driven control of wave energy systems. In *Trends in Renewable Energies Offshore*, 401–409. CRC Press, London. doi:10.1201/9781003360773-46.

Peña-Sanchez, Y., Faedo, N., Penalba, M., Giorgi, G., Merigaud, A., Windt, C., Wang, L., Ringwood, J., and García Violini, D. (2019). Finite-Order hydrodynamic Approximation by Moment-Matching (FOAMM) toolbox for wave energy applications. In *13th European Wave and Tidal Energy Conference (EWTEC)*. Napoli, Italy.

Peña-Sanchez, Y., Windt, C., Davidson, J., and Ringwood, J.V. (2020). A Critical Comparison of Excitation Force Estimators for Wave-Energy Devices. *IEEE Transactions on Control Systems Technology*, 28(6), 2263–2275. doi:10.1109/TCST.2019.2939092.

Penalba, M., Giorgi, G., and Ringwood, J.V. (2017). Mathematical modelling of wave energy converters: A review of nonlinear approaches. *Renewable and Sustainable Energy Reviews*, 78, 1188–1207. doi:10.1016/j.rser.2016.11.137.

Ringwood, J.V. (2020). Wave energy control: status and perspectives 2020. *IFAC-PapersOnLine*, 53(2), 12271–12282. doi:10.1016/j.ifacol.2020.12.1162.

Schoukens, J. and Ljung, L. (2019). Nonlinear System Identification: A User-Oriented Road Map. *IEEE Control Systems*, 39(6), 28–99. doi:10.1109/MCS.2019.2938121.

Zhang, Y., Zeng, T., and Li, G. (2020). Robust Excitation Force Estimation and Prediction for Wave Energy Converter M4 Based on Adaptive Sliding-Mode Observer. *IEEE Transactions on Industrial Informatics*, 16(2), 1163–1171. doi:10.1109/TII.2019.2941886.